

## Mucoadhesion of polystyrene nanoparticles having surface hydrophilic polymeric chains in the gastrointestinal tract

Shinji Sakuma <sup>a,\*</sup>, Rika Sudo <sup>a</sup>, Norio Suzuki <sup>a</sup>, Hiroshi Kikuchi <sup>a</sup>, Mitsuru Akashi <sup>b</sup>, Masahiro Hayashi <sup>c</sup>

<sup>a</sup> *Pharmaceutical Formulation Research Laboratory, Daiichi Pharmaceutical Co., Ltd., Kita-Kasai, Edogawa-ku, Tokyo 134-8630, Japan*

<sup>b</sup> *Department of Applied Chemistry and Chemical Engineering, Faculty of Engineering, Kagoshima University, Korimoto, Kagoshima 890-0065, Japan*

<sup>c</sup> *Faculty of Pharmaceutical Sciences, Science University of Tokyo, Ichigaya Funagawara-machi, Shinjuku-ku, Tokyo 162-0826, Japan*

Received 9 April 1998; received in revised form 10 June 1998; accepted 12 October 1998

---

### Abstract

The mucoadhesion of polystyrene nanoparticles having surface hydrophilic polymeric chains in the gastrointestinal (GI) tract was investigated in rats. Radiolabeled nanoparticles were synthesized by adding hydrophobic 3-(trifluoromethyl)-3-(*m*-[<sup>125</sup>I]iodophenyl)diazirine in the final process of nanoparticle preparation. The radioiodinated diazirine seemed to be incorporated in the hydrophobic polystyrene core of nanoparticles. The incorporation rate was less than 10%, irrespective of nanoparticle type. The diazirine incorporated in nanoparticles exhibited little leakage from them even though they were mixed with a solution corresponding to GI juice. The change in blood ionized calcium concentration after oral administration of salmon calcitonin (sCT) with nanoparticles showed that the *in vivo* enhancement of sCT absorption by radiolabeled nanoparticles was the same as that by non-labeled nanoparticles. The GI transit rates of nanoparticles having surface poly(*N*-isopropylacrylamide), poly(vinylamine) and poly(methacrylic acid) chains, which can improve sCT absorption, were slower than that of nanoparticles covered by poly(*N*-vinylacetamide), which does not enhance sCT absorption at all. These slow transit rates were probably the result of mucoadhesion of nanoparticles. The strength of mucoadhesion depended on the structure of the hydrophilic polymeric chains on the nanoparticle surface. The mucoadhesion of poly(*N*-isopropylacrylamide) nanoparticles, which most strongly enhanced sCT absorption, was stronger than that of ionic nanoparticles, and poly(*N*-vinylacetamide) nanoparticles probably did not adhere to the GI mucosa. These findings demonstrated that there is a good correlation between mucoadhesion and enhancement of sCT absorption. © 1999 Elsevier Science B.V. All rights reserved.

**Keywords:** Nanoparticle; Absorption enhancement; Peptide; Mucoadhesion; Bioadhesion; Gastrointestinal tract

---

\* Corresponding author. Tel.: +81-3-5696-8154; fax: +81-3-5696-8466; e-mail: sakumv8j@daiichipharm.co.jp.

## 1. Introduction

Polystyrene nanoparticles having surface hydrophilic polymeric chains have been developed using free radical copolymerization between hydrophilic macromonomers and hydrophobic styrene (Akashi et al., 1985, 1989, 1990; Riza et al., 1994, 1995; Chen et al., 1996). We have investigated the potential of these nanoparticles as carriers for oral peptide delivery using salmon calcitonin (sCT) in rats. The decrease in blood ionized calcium concentration and the increase in plasma sCT concentration after oral administration of sCT with nanoparticles demonstrated that these nanoparticles enhanced sCT absorption via the gastrointestinal (GI) tract (Sakuma et al., 1997a,b). This absorption enhancement was affected by the chemical structure of the hydrophilic polymeric chains, which are located on the nanoparticle surface, and sCT absorption was enhanced most strongly by nanoparticles having thermosensitive nonionic poly(*N*-isopropylacrylamide) (PNIPAAm) chains on their surfaces. The absorption of sCT was also enhanced by nanoparticles with surface cationic poly(vinylamine) (PVAm) or anionic poly(methacrylic acid) (PMAA) chains, although enhancement was weaker than that with PNIPAAm nanoparticles. However, there was no absorption enhancement of sCT by nonionic poly(*N*-vinylacetamide) (PNVA) nanoparticles.

We hypothesized that the absorption enhancement of sCT by these nanoparticles resulted mainly from both bioadhesion of nanoparticles incorporating sCT to the GI mucosa and an increase in the stability of sCT in the GI tract (Sakuma et al., 1997a). The stabilizing effect of nanoparticles on the enzymatic degradation of sCT has already been examined *in vitro* (Sakuma et al., 1997c), and it has been confirmed that nanoparticles protect sCT against digestive enzyme-catalyzed degradation and that this stabilizing effect is affected by macromonomer structure. In addition, there was a good correlation between this *in vitro* stability of sCT in the presence of nanoparticles and the ranking of the effectiveness of nanoparticles for enhancing the *in vivo* absorption of sCT. These findings demonstrated that

nanoparticles stabilize peptide drugs in the GI tract, and that this property affects the absorption enhancement of orally administered sCT.

On the other hand, many researchers have reported that mucoadhesive polymers improve the bioavailability of drugs with poor absorption characteristics (Longer et al., 1985; Kreuter, 1991; Lehr et al., 1990, 1992; Takeuchi et al., 1996). We also consider that the mucoadhesion of nanoparticles in the GI tract contributes to the enhancement of sCT absorption. However, there is no sufficient data concerning with the mucoadhesion although it has been already suggested that PNIPAAm nanoparticles have the property of adhering to the gastric mucosa (Sakuma et al., 1997b). In this study, we examined the effect of the chemical structure of nanoparticles on their mucoadhesion in the GI tract and the strength of mucoadhesion, and discussed the correlation between mucoadhesion of nanoparticles and enhancement of sCT absorption *in vivo*.

## 2. Materials and methods

### 2.1. Materials

Deoxycholic acid and sCT were purchased from Sigma Chemical Co. (St. Louis, MO, USA). 3-(Trifluoromethyl)-3-(*m*-[<sup>125</sup>I]iodophenyl)diazirine, 370 GBq/mmol, was obtained from Amersham International plc. (Bucks, UK). Tritiated polyethylene glycol (PEG) with number-average molecular weight 4000, 18.5–74.0 MBq/g, was purchased from Daiichi Pure Chemical Co. (Tokyo, Japan). *N*-vinylacetamide (NVA) monomer was supplied by Showa Denko Co. (Tokyo, Japan). *N*-isopropylacrylamide (NIPAAm) and *t*-butyl methacrylate (BMA) monomers were obtained from Kohjin Co. (Tokyo, Japan). *p*-Chloromethyl styrene (*p*-CMSt) was furnished by Nippon Oil and Fats Co. (Tokyo, Japan). All other chemicals were commercial products of reagent grade. These materials were purified in the usual manner when necessary (Riza et al., 1995; Chen et al., 1996; Sakuma et al., 1997a).

## 2.2. Preparation of nanoparticles

PNIPAAm, PNVA, PVAm and PMAA nanoparticles were prepared using the procedures reported in our earlier article (Sakuma et al., 1997a). Oligomerization of each monomer, initiated by 2,2'-azobisisobutyronitrile (AIBN), was carried out in the presence of 2-mercaptoethanol to give oligomers terminating in hydroxyl groups. These oligomers were condensed with *p*-CMSt to obtain macromonomers terminating in vinylbenzyl groups. After dispersion copolymerization initiated by AIBN between the macromonomers and styrene, nonionic PNIPAAm, PNVA and polyBMA (PBMA) nanoparticles were obtained. PVAm and PMAA nanoparticles were prepared by the hydrolysis of PNVA and PBMA nanoparticles, respectively. The resulting nanoparticles were dialyzed to remove unreacted substances, and then lyophilized.

Separately, radiolabeled nanoparticles were prepared using 3-(trifluoromethyl)-3-(*m*-[<sup>125</sup>I]iodophenyl)diazirine, as follows. The macromonomers, styrene and AIBN (less than 1 mol% to monomer) were dissolved in 2.5 ml of ethanol. The molar concentration of styrene was 40-fold that of macromonomers, and the total amount of the macromonomers and styrene was 500 mg. Three hundred and seventy kBq of the radioiodonated diazirine dissolved in 0.25 ml of ethanol was added to the ethanol solution containing macromonomers. After dispersion copolymerization between macromonomers and styrene at 60°C in a vacuum for 8 h, PNIPAAm, PNVA and PBMA nanoparticles incorporating radioiodonated diazirine were obtained. The resulting radiolabeled nanoparticles were dialyzed in ethanol using a cellulose dialyzed tube to remove radioiodonated diazirine not incorporated in nanoparticles. The radiolabeled nonionic PNIPAAm and PNVA nanoparticles were hydrolyzed in 4 N hydrochloric acid (HCl) at 80°C for 24 h in order to replace NVA with VAm on the nanoparticle surface. After hydrolysis, the radiolabeled PVAm nanoparticles were dialyzed in purified water. The radiolabeled anionic PMAA nanoparticles were prepared by hydrolyzing the radiolabeled PBMA nanoparticles in ethanol contain-

ing 4 N HCl at 80°C for 24 h so as to replace BMA with MAA. After dialysis of these PMAA nanoparticles in ethanol, they were further dialyzed in purified water.

## 2.3. Characterization

### 2.3.1. Number-average molecular weight of macromonomers

The number-average molecular weight ( $M_n$ ) of macromonomers on the nanoparticle surface was determined by gel permeation chromatography (Sakuma et al., 1997a).

### 2.3.2. Nanoparticle size

The particle size of the non-labeled nanoparticles was measured by dynamic light-scattering spectrophotometry (DLS-700, Otsuka Electronics Co., Japan).

### 2.3.3. Rate of radioiodonated diazirine incorporated in nanoparticles

The total volume (ml) of the radiolabeled nanoparticle aqueous dispersion just after the dialysis described in Section 2.2 was measured. One ml of the nanoparticle aqueous dispersion was centrifuged at 15 000 rpm for 30 min at 25°C. After removal of the supernatant, the radioactivity of the precipitated nanoparticles was measured with a gamma counter (ARC-1000M, Aloka Co., Japan). The rate of radioiodonated diazirine incorporated in nanoparticles was calculated from the total radioactivity of the nanoparticle aqueous dispersion and the additional amount of radioiodonated diazirine in the copolymerization (370 kBq).

### 2.3.4. Leakage of radioiodonated diazirine from nanoparticles

A male Sprague–Dawley (SD) strain rat weighting 220 g was sacrificed by ether inhalation overdose, and the stomach and small intestine were removed. The lumens of the stomach and the intestine were rinsed in 10 ml of a HCl–sodium chloride (HCl–NaCl) buffered solution (pH 1.2; ionic strength: 0.1) and a phosphate buffered solution (pH 6.8; ionic strength: 0.1), respectively.

The radiolabeled nanoparticle aqueous dispersion (0.1 ml) was mixed with 0.9 ml of purified water, the HCl–NaCl buffered solution with or without the gastric contents, or the phosphate buffered solution with or without the intestinal contents. These samples were incubated at 37°C for 2 h and centrifuged at 15 000 rpm for 30 min at 25°C. The amount of radioiodinated diazirine in the supernatant was measured by gamma scintigraphy.

#### 2.3.5. Absorption enhancement of sCT by radiolabeled nanoparticles

The concentration of the radiolabeled nanoparticles dispersed in purified water, was adjusted to 20 mg/ml. This dispersion was mixed with sCT dissolved in purified water. The concentrations of sCT and nanoparticles in this mixture were adjusted to 0.1 and 10 mg/ml, respectively.

The animal experiments were carried out in the same manner as described in our previous study (Sakuma et al., 1997a). Briefly, male SD strain rats (three per group) weighing 200–240 g were fasted overnight with free access to water before the *in vivo* study. A mixture of sCT and nanoparticles was given orally to rats at a dose of 0.25 mg of sCT and 25 mg of nanoparticles in a 2.5 ml mixture/kg of body weight. As a control, an aqueous solution of sCT was administered to rats under the same conditions. The ionized calcium concentration in blood obtained from the tail vein was measured, and the change in calcium concentration from before to after oral administration of the dosing solution was calculated.

### 2.4. Distribution of nanoparticles in the GI tract

#### 2.4.1. Dosing solution

The radiolabeled nanoparticles were mixed with non-labeled nanoparticles. The final nanoparticle concentration and the radioactivity in this mixture were adjusted to 10 mg/ml and 0.3–0.5 kBq/ml, respectively. As a control solution, an aqueous solution of PEG was prepared. The concentration of non-labeled PEG was adjusted to 10 mg/ml and a small amount of tritiated PEG was added to this solution, to yield 0.3–0.5 kBq/ml.

#### 2.4.2. *In vivo* study

The dosing solution was given orally to male SD strain rats fasted overnight (weight: 200–240 g,  $n = 5$ ) at a dose of 25 mg of nanoparticles in a 2.5 ml solution/kg of body weight. PEG aqueous solution was administered to rats under the same conditions. At 5 min, 30 min, 1 or 2 h after administration, rats were sacrificed by ether inhalation overdose, and the stomach and small intestine were removed. The intestine was cut into 10-cm sections. The radioactivity in each segment was measured with the gamma counter or a beta counter (Beckman, LS6000TA, Fullerton, CA, USA).

#### 2.4.3. Analysis

The transit of nanoparticles through the GI tract was evaluated using a modification of the kinetic model designed by Akiyama et al. (1995), as shown in Fig. 1. It was assumed that nanoparticles were emptied from the stomach and moved through each segment of the intestine with zero-order kinetics. The gastric emptying rate was defined as  $k_1$ . The respective segments of the small intestine were divided into upper (0–60 cm of the intestine) and lower parts (60–110 cm of the intestine). The amount of nanoparticles in each compartment was estimated from the radioactivity measured in Section 2.4.2. The transit rate of nanoparticles through the intestinal tract was defined as  $k_2$ . Each rate constant was calculated using the non-linear least-squares method with a weight of 1 (MULTI) (Yamaoka et al., 1981).

### 2.5. Mucoadhesion of nanoparticles in the intestinal tract

#### 2.5.1. Dosing solution

The radiolabeled nanoparticles were centrifuged at 15 000 rpm for 30 min at 25°C, removed super-

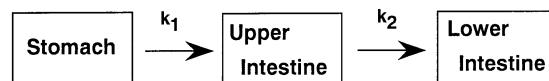


Fig. 1. Kinetic model of nanoparticles in the GI tract. Nanoparticle gastric emptying rate and intestinal transit rate were defined as  $k_1$  and  $k_2$ , respectively. It was assumed that nanoparticles moved through the GI tract with zero-order kinetics.

nant and redispersed in the phosphate buffered solution of pH 6.8. The lyophilized non-labeled nanoparticles were dispersed in the same phosphate buffered solution. These nanoparticle dispersions were mixed, and the concentration and the radioactivity of this mixture were adjusted to 10 mg/ml and 0.3–0.5 kBq/ml, respectively.

### 2.5.2. *In vivo* study

Male SD strain rats fasted overnight (weight: 200–220 g,  $n = 3$ ) were anaesthetised with urethane and the abdomen was opened along the median line. Tygon<sup>®</sup> tubings were inserted in the small intestine just below Treitz' ligament and the intestine 10 cm below Treitz' ligament, and each position was ligated. At 5 min after injection of the dosing solution into this loop at a dose of 10 mg of nanoparticles in a 1 ml solution/kg of body weight, the phosphate buffered solution previously heated to 37°C was perfused for 10 min at 1 ml/min. After dissection of the loop, the amount of nanoparticles remaining in the intestinal lumen was calculated from the radioactivities in the loop and the perfusate. Statistical significance was assessed with Student's *t*-test, and *P* values of 0.05 or less were considered significant.

After perfusion by the phosphate buffered solution, 5 w/v% deoxycholic acid aqueous solution (37°C) was subsequently perfused for 30 min at 1 ml/min to remove the mucous layer. As a control, physiological saline was perfused under the same conditions. The radioactivity in each perfusate was measured by gamma scintigraphy.

## 3. Results

### 3.1. Preparation of nanoparticles

#### 3.1.1. Non-labeled nanoparticles

Fig. 2 and Table 1 show the chemical structures and the characteristics of the nanoparticles not incorporating radiolabeled diazine, respectively. These characteristics were the same as those described in our previous study (Sakuma et al., 1997a). Briefly, the number-average molecular weight of macromonomers on the nanoparticle surface was adjusted to the order of  $10^3$ , the

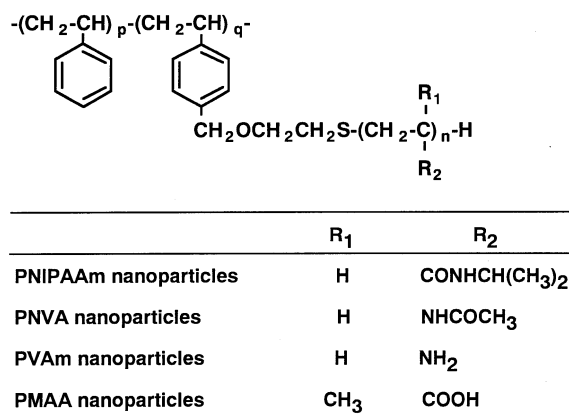


Fig. 2. Chemical structures of nanoparticles.

weight-average diameter of nanoparticles was less than 1000 nm, and all nanoparticles possessed good water-dispersibility.

#### 3.1.2. Radiolabeled nanoparticles

Water-dispersible radiolabeled nanoparticles were prepared by adding radioiodinated diazine in the dispersion copolymerization between macromonomers and styrene. Table 2 shows the rates of radioiodinated diazine incorporated in nanoparticles and leakage from nanoparticles into the respective solutions. The incorporation rate was less than 10%, irrespective of nanoparticle type. However, radioiodinated diazine was not detected in the dispersion medium at all after purification (data not shown). After incubation of

Table 1  
Characteristics of non-labeled nanoparticles

	$M_n^a$	$M_w/M_n^b$	Diameter (nm) <sup>c</sup>
PNIPAAm nanoparticles	5.2	2.1	440
PNVA nanoparticles	5.2	2.1	380
PVAm nanoparticles	5.2	2.1	360
PMAA nanoparticles	3.9	2	500

<sup>a</sup> Number-average molecular weight of macromonomers ( $\times 10^{-3}$ ).

<sup>b</sup> Weight-average molecular weight ( $M_w$ )/number-average molecular weight ( $M_n$ ) ratio.

<sup>c</sup> Weight-average diameter.

Table 2  
 Characteristics of radiolabeled nanoparticles incorporating radioiodinated diazirine

	Incorporated (%) <sup>a</sup>	Leakage (%) <sup>b</sup>				
		Purified water	HCl–NaCl solution <sup>c</sup>	Phosphate solution <sup>d</sup>	Gastric solution <sup>e</sup>	Intestinal solution <sup>f</sup>
PNIPAAm nanoparticles	6.4	0.6	0.6	0.9	0.2	0.1
PNVA nanoparticles	4.6	0.3	0.4	0.9	0.4	0.8
PVAm nanoparticles	2.8	0	0.2	0.4	1.3	1.1
PMAA nanoparticles	7.9	0	0.9	0	0.8	0.2

<sup>a</sup> Rate of radioiodinated diazirine incorporated in nanoparticles.

<sup>b</sup> Rate of radioiodinated diazirine leakage from radiolabeled nanoparticles 2 h after incubation.

<sup>c</sup> Hydrochloric acid–sodium chloride buffered solution (pH 1.2; ionic strength: 0.1).

<sup>d</sup> Phosphate buffered solution (pH 6.8; ionic strength: 0.1).

<sup>e</sup> Hydrochloric acid–sodium chloride buffered solution with rat's gastric contents.

<sup>f</sup> Phosphate buffered solution with rat's small intestinal contents.

these radiolabeled nanoparticles with the respective solutions at 37°C for 2 h, about 1% of the radioiodinated diazirine incorporated in nanoparticles leaked from them. Fig. 3 shows the change in blood ionized calcium concentration after oral administration of the mixture of sCT and radiolabeled nanoparticles. The decrease in calcium concentration was greater than that after oral administration of sCT aqueous solution, except for the case of PNVA nanoparticles. It was confirmed that the order of enhancement by nanoparticles of sCT absorption via the GI tract was PNIPAAm, PVAm and PMAA nanoparticles, as was the case of non-labeled nanoparticles (Sakuma et al., 1997a).

### 3.2. Distribution of nanoparticles in the GI tract

Fig. 4 shows the amounts of nanoparticles in the stomach and intestinal segments at 5, 30 min, 1 and 2 h after oral administration of aqueous dispersion of non-labeled and radiolabeled nanoparticles. Kinetic parameters of nanoparticles in the GI tract are listed in Table 3. In this case, sCT did not affect the transit rates of nanoparticles (data not shown). PNIPAAm, PVAm and PMAA nanoparticles clearly remained in the stomach, and their gastric emptying rates were less than 1% of dose/min. The transit rates

of these nanoparticles through the intestinal tract were less than 0.5% of dose/min. On the other hand, the gastric emptying rate and the intestinal transit rate of PNVA nanoparticles were higher than those of the other nanoparticles and nearly equal to those of PEG which does not adhere to the GI mucosa (Junginger, 1990).

### 3.3. Mucoadhesion of nanoparticles in the intestinal tract

We next examined the mucoadhesion of nanoparticles that remained in the GI tract for a long period of time, using the in situ intestinal perfusion technique. Fig. 5 shows the residual amounts of nanoparticles in the intestinal lumen after perfusion with the phosphate buffered solution. More than 50% of PVAm and PMAA nanoparticles were eluted from the intestine with the phosphate buffered solution, although more than 80% of PNIPAAm nanoparticles remained in the intestinal lumen after perfusion. The differences in the residual amounts between PNIPAAm nanoparticles and both types of ionic nanoparticles were significant. However, there was no significant difference between residual amounts of the two ionic nanoparticles.

On the other hand, when the mucous layer was removed with deoxycholic acid, many PNIPAAm-

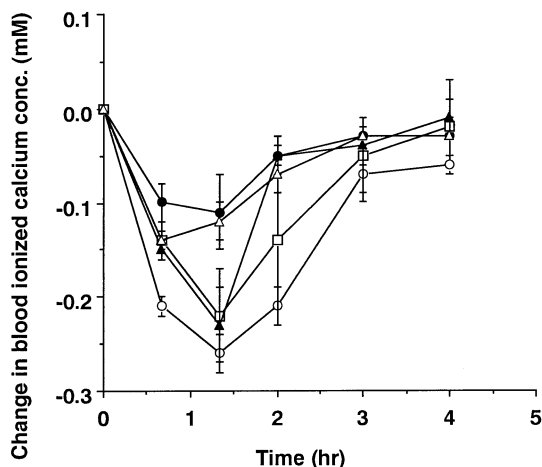


Fig. 3. Concentration-time profiles of ionized calcium in blood after oral administration of sCT aqueous solution (●), a mixture of sCT and PNIPAAm nanoparticles (○), a mixture of sCT and PNVA nanoparticles (△), a mixture of sCT and PVAm nanoparticles (□) and a mixture of sCT and PMAA nanoparticles (▲) in rats (0.25 mg sCT with 25 mg nanoparticles in 2.5 ml dosing solution/kg rat). The radioiodinated diazirine was incorporated in nanoparticles. Each value represents the mean  $\pm$  S.E ( $n = 3$ ).

nanoparticles that had remained in the intestinal lumen after perfusion with the phosphate buffered solution were eluted from the intestine (Fig. 6). The removal of the intestinal mucous layer was confirmed by the increase in concentration of protein arising from the mucous layer in the perfusate (data not shown). Based on the findings

shown in Figs. 5 and 6, the amount of PNIPAAm nanoparticles eluted with deoxycholic acid was estimated to be about 60% of that remaining in the intestinal lumen after perfusion with the phosphate buffered solution. This amount was 10-fold that of physiological saline.

#### 4. Discussion

It has been reported that some mucoadhesive polymers improve the bioavailability of drugs with poor absorption characteristics (Longer et al., 1985; Kreuter, 1991; Pimienta et al., 1990). Lehr et al. (1990, 1992) found that the in vitro absorption of a vasopressin derivative through rat intestine was enhanced by mucoadhesive poly-(acrylic) acid crosslinked by divinylglycol. Takeuchi et al. (1996) studied the effect of chitosan, which is a mucoadhesive cationic polymer, on the intestinal absorption of insulin in rats, and found that blood glucose concentration decreased significantly after oral administration of insulin-loaded chitosan-coated liposomes. It is generally accepted that bioadhesive polymers can increase the drug concentration in the vicinity of the intestinal epithelial cells through intensifying the contact of drugs with the intestinal mucosa, and can consequently enhance the drug absorption via the intestinal tract. Kreuter (1991) and Couvreur and Puisieux (1993) have proposed that mucoadhesion of colloidal carriers is one of the important properties for improving the bioavailability of poor absorptive drugs by them. We also consider that the enhancement effect of peptide absorption is caused by the interaction between nanoparticles incorporating peptide and the GI mucosa, in addition to the stabilizing effect of nanoparticles on the enzymatic degradation of peptide (Sakuma et al., 1997c).

In the present study, nanoparticles incorporating radiolabeled diazirine were used to demonstrate the mucoadhesion of nanoparticles in the GI tract. Radioiodinated diazirine is a hydrophobic compound which is often used to selectively radiolabel the hydrophobic lipid phase of membranes (Brunner and Semenza, 1981). It seemed that this radioiodinated compound interacted

Table 3  
Kinetic parameters of nanoparticles in the GI tract

	Gastric emptying rate ( $k_1$ , % of dose/min)	Transit rate through intestinal tract ( $k_2$ , % of dose/min)
PNIPAAm nanoparticles	0.62	0.39
PNVA nanoparticles	1.42	1.26
PVAm nanoparticles	0.35	0.23
PMAA nanoparticles	0.87	0.44
Control <sup>a</sup>	1.67	1.32

<sup>a</sup> PEG aqueous solution ( $M_n$ : 4000).

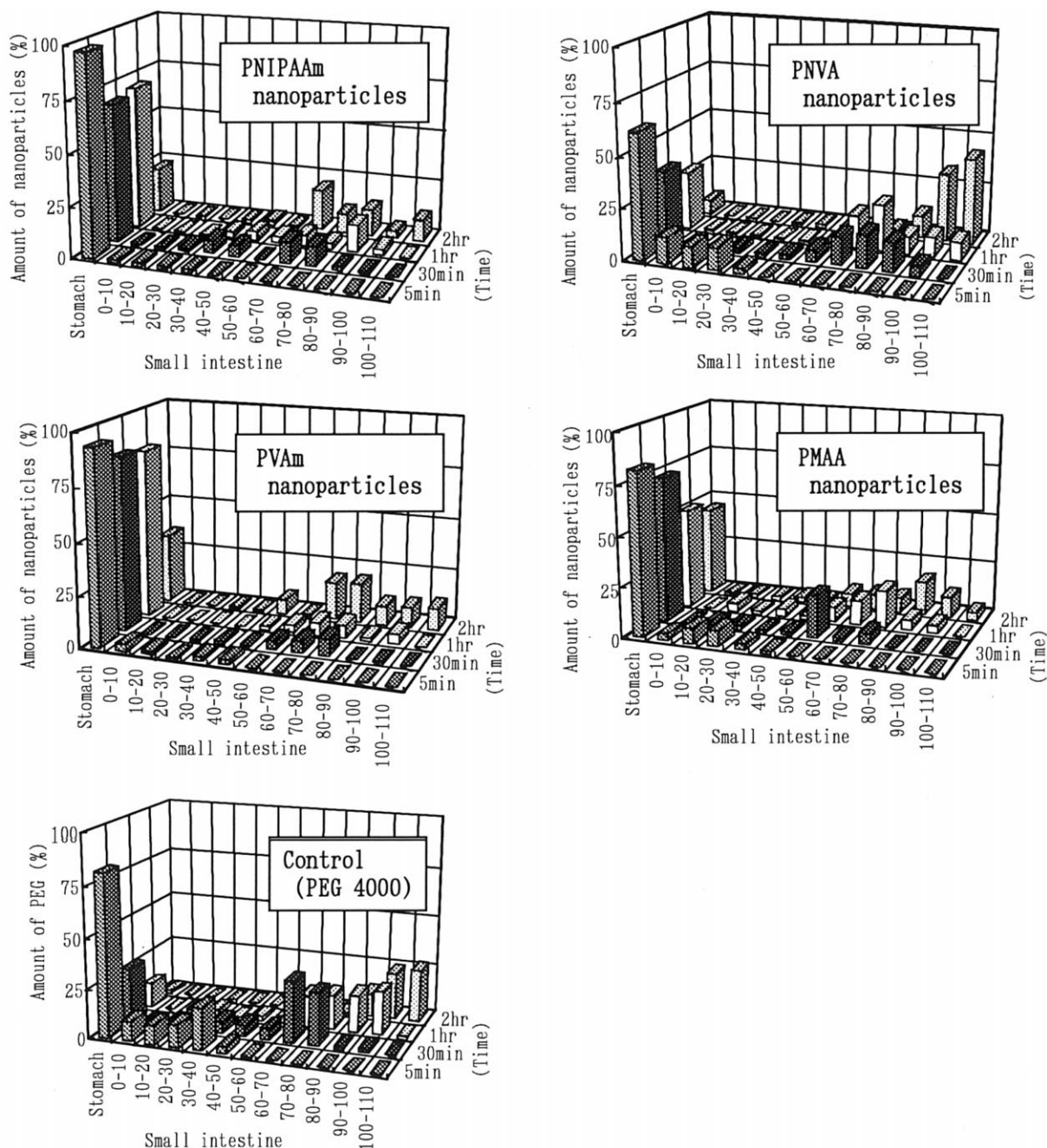


Fig. 4. Distribution of nanoparticles in the GI tract after oral administration of nanoparticle aqueous dispersion or PEG aqueous solution (25 mg nanoparticles or PEG in 2.5 ml dosing solution/kg rat). The radioactivity of the dosing solution was adjusted to 0.3–0.5 kBq/ml. At 5 min, 30 min, 1 or 2 hr after administration, rats were sacrificed by ether inhalation overdose, and the stomach and small intestine were removed. The intestine was cut into 10-cm sections. The radioactivity in stomach and each intestinal segment was measured by gamma or beta scintigraphy. Each value represents the mean of results of five experiments.

with hydrophobic styrene in the dispersion copolymerization, and that it was consequently incorporated in the hydrophobic polystyrene core of nanoparticles, although the rate of this incorporation was low. However, radioiodinated diazidine incorporated in nanoparticles exhibited little leakage from them even though they were diluted with a solution corresponding to GI juice (Table 2). In addition, the enhancement of sCT absorption by radiolabeled nanoparticles shown in Fig. 3 was the same as that by non-labeled nanoparticles (Sakuma et al., 1997a). These findings imply that the characteristics of nanoparticles is hardly affected by radiolabeling, and that the behavior of nanoparticles in the GI tract can be estimated by the radioactivity of radioiodinated diazidine.

As is clear from Fig. 4 and Table 3, the gastrointestinal transit rates of nanoparticles having

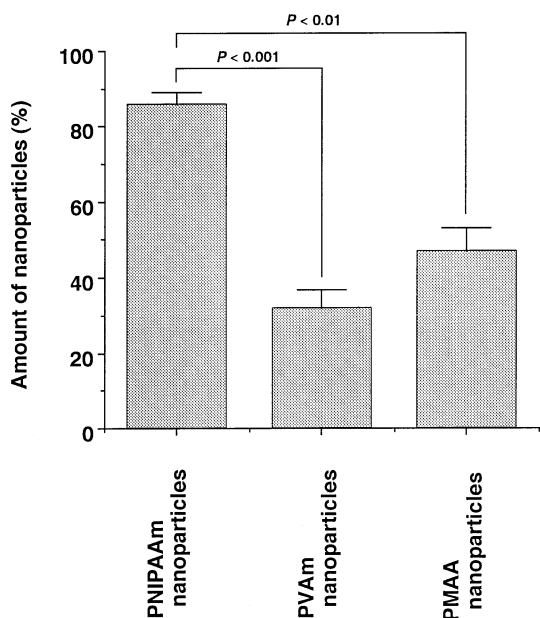


Fig. 5. Amounts of nanoparticles remaining in the intestinal lumen. Rats were anaesthetised with urethane, and nanoparticles dispersed in a phosphate buffered solution of pH 6.8 were injected into the 10-cm intestinal loop (10 mg of nanoparticles in 1 ml dosing solution/kg rat). The radioactivity of the dosing solution was adjusted to 0.3–0.5 kBq/ml. At 5 min after injection, the phosphate buffered solution was perfused for 10 min at 1 ml/min. The radioactivities of the dissected loop and the perfusate were measured by gamma scintigraphy. Each value represents the mean  $\pm$  S.E ( $n = 3$ ).

surface PNIPAAm, PVAm or PMAA chains, which can improve sCT absorption via the GI tract, were slower than that of PNVA nanoparticles which does not enhance sCT absorption at all. These gastric emptying patterns of nanoparticles were almost the same as those analyzed monoexponentially (data not shown). In either case, there was a good fit between the observed and calculated values. In addition, Fig. 6 showed directly that PNIPAAm nanoparticles remained in the intestinal lumen due to the interaction between nanoparticles and the mucous layer. The slow transit rates of PNIPAAm, PVAm and PMAA nanoparticles in the GI tract were probably the result of this mucoadhesion of nanoparticles. The similar transit rates through the GI tract between PNVA nanoparticles and PEG suggested that there was no interaction between PNVA

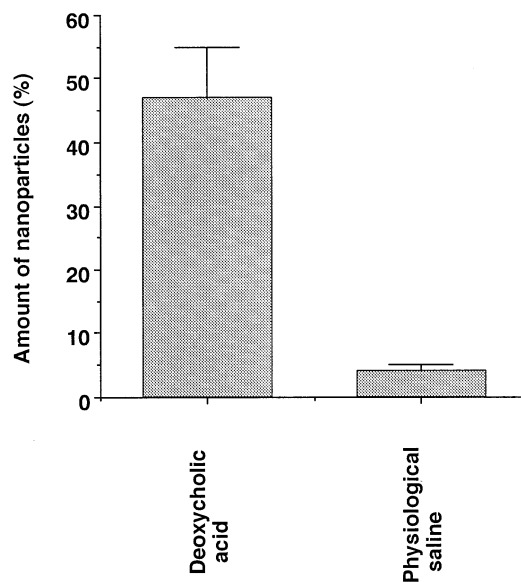


Fig. 6. Amounts of PNIPAAm nanoparticles in perfusate. Rats were anaesthetised with urethane, and nanoparticles dispersed in a phosphate buffered solution of pH 6.8 were injected into the 10-cm intestinal loop (10 mg of nanoparticles in 1 ml dosing solution/kg rat). The radioactivity of the dosing solution was adjusted to 0.3–0.5 kBq/ml. At 5 min after injection, the phosphate buffered solution was perfused for 10 min at 1 ml/min. Deoxycholic acid aqueous solution (5 w/v%) and physiological saline were subsequently perfused for 30 min at 1 ml/min, respectively. The radioactivity of each perfusate was measured by gamma scintigraphy. Each value represents the mean  $\pm$  S.E ( $n = 3$ ).

nanoparticles and the mucous layer. Findings obtained using the *in situ* intestinal perfusion technique also indicated that the strength of mucoadhesion depended on the structure of the hydrophilic polymeric chains on the nanoparticle surface (Fig. 5). In this experiment, when nanoparticles do not adhere to the intestinal mucosa or only weakly interact with the mucous layer, they are probably readily eluted from the intestinal lumen with the perfusate. Fig. 5 suggested that the mucoadhesion of PNIPAAm nanoparticles is stronger than that of the ionic nanoparticles, although it may be necessary to review the mucoadhesion of nanoparticles by other *in vitro* method.

These results demonstrate that there is a good correlation between the mucoadhesion of nanoparticles and their *in vivo* enhancement of sCT absorption and that this mucoadhesion depends on the chemical structure of the hydrophilic polymeric chains on the nanoparticle surface. It was predicted that the mucoadhesion is hardly affected by the particle size and the molecular weight of the surface polymeric chains, because the enhancement effect of sCT absorption by PNIPAAm nanoparticles was constant, irrespective of above-mentioned characteristics of nanoparticles (Sakuma et al., 1997a). PNIPAAm, PVAm and PMAA nanoparticles perhaps adhered to the GI mucosa by electrostatic interaction, hydrophobic interaction, or hydrogen bonding (Gu et al., 1988; Takeuchi et al., 1996; Sakuma et al., 1997a). However, there is no evidence that drug incorporated in nanoparticles accumulated in the vicinity of the intestinal epithelial cells to improve its absorption. We are now directly studying the effect of mucoadhesion of nanoparticles on sCT absorption, using the *in vitro* everted sac technique.

On the other hand, when the mechanism of the absorption enhancement of peptide by nanoparticles is discussed, the stabilizing effect of nanoparticles on the enzymatic degradation of peptides reported in our previous study must be considered (Sakuma et al., 1997c). The mutual contribution of mucoadhesion and stabilizing

effect remains to be examined. The explanation of this balance most likely promotes the development of novel nanoparticles inducing the excellent enhancement effect of peptide absorption. The enhancement effect probably increases by decreasing the amount of nanoparticles adhered to the gastric mucosa because most of drugs including sCT are absorbed from the intestinal membrane (Sakuma et al., 1997b). In addition, it may be necessary to examine the uptake of nanoparticles by Peyer's patches (Florence et al., 1995) and the opening of tight junctions between intestinal epithelial cells by nanoparticles (Borchard et al., 1996). Further work will be successively described in future reports.

## 5. Conclusions

The bioadhesion of polystyrene nanoparticles having surface hydrophilic polymeric chains to the GI mucosa was investigated using radiolabeled nanoparticles incorporating 3-(trifluoromethyl)-3-(*m*-[<sup>125</sup>I]iodophenyl)diazirine in their polystyrene core. The radioiodinated diazirine incorporated in nanoparticles exhibited little leakage from them, although its incorporation rate was less than 10%. The order of enhancement by radiolabeled nanoparticles of sCT absorption via the GI tract was PNIPAAm, PVAm and PMAA nanoparticles, as was the case of non-labeled nanoparticles. The GI transit rates of PNIPAAm, PVAm and PMAA nanoparticles were slower than that of PNVA nanoparticles, which does not enhance sCT absorption at all. These slow transit rates were probably the result of mucoadhesion of nanoparticles. The strength of mucoadhesion depended on the structure of surface polymeric chains, and PNIPAAm nanoparticles exhibited the strongest mucoadhesion. In addition, it was suggested that there was no interaction between PNVA nanoparticles and the mucous layer. These results demonstrated that there is a good correlation between mucoadhesion and enhancement of sCT absorption.

## Acknowledgements

This work was financially supported in part by a Grant-in-Aid for Scientific Research in Priority Areas of 'New Polymers and Their Nano-Organized Systems' (No.277/08246243) from the Ministry of Education, Science, Sports and Culture of Japan. The authors are very grateful to Dr Akio Kishida and Dr Takeshi Serizawa for their helpful comments, and to Ken-ichiro Hiwatari for the synthesis of macromonomers. We also appreciate Dr Kiyoto Yachi's aid in the analysis of kinetic parameters of nanoparticles in the GI tract.

## References

- Akashi, M., Kirikihara, I., Miyauchi, N., 1985. Synthesis and polymerization of a styryl terminated oligovinylpyrrolidone macromonomer. *Angew. Macromol. Chem.* 132, 81–89.
- Akashi, M., Yanagi, T., Yashima, E., Miyauchi, N., 1989. Graft copolymers having hydrophobic backbone and hydrophilic branches, IV. A copolymerization study of water-soluble oligovinylpyrrolidone macromonomers. *J. Polym. Sci. Polym. Chem.* 27, 3521–3530.
- Akashi, M., Chao, D., Yashima, E., Miyauchi, N., 1990. Graft copolymers having hydrophobic backbone and hydrophilic branches, V. Microspheres obtained by the copolymerization of poly(ethylene glycol) macromonomer with methyl methacrylate. *J. Appl. Polym. Sci.* 39, 2027–2030.
- Akiyama, Y., Nagahara, N., Kashiwara, T., Hirai, S., Toguchi, H., 1995. In vitro and in vivo evaluation of mucoadhesive microspheres prepared for the gastrointestinal tract using polyglycerol esters of fatty acids and a poly(acrylic acid) derivative. *Pharm. Res.* 12, 397–405.
- Borchard, G., Lußen, H.L., de Boer, A.G., Verhoef, J.C., Lehr, C.M., Junginger, H.E., 1996. The potential of mucoadhesive polymers in enhancing intestinal peptide drug absorption. III: effects of chitosan-glutamate and carbomer on epithelial tight junctions in vitro. *J. Control. Rel.* 39, 131–138.
- Brunner, J., Semenza, G., 1981. Selective labeling of the hydrophobic core of membranes with 3-(trifluoromethyl)-3-(*m*-<sup>125</sup>Iiodophenyl) diazine, a carbene-generating reagent. *Biochemistry* 20, 7174–7182.
- Chen, M.Q., Kishida, A., Akashi, M., 1996. Graft copolymers having hydrophobic backbone and hydrophilic branches, XI. Preparation and thermosensitive properties of polystyrene microspheres having poly(*N*-isopropylacrylamide) branches on their surfaces. *J. Polym. Sci. Polym. Chem.* 34, 2213–2220.
- Couvreur, P., Puisieux, F., 1993. Nano- and microparticles for the delivery of polypeptides and proteins. *Adv. Drug Deliv. Rev.* 10, 141–162.
- Florence, A.T., Hillery, A.M., Hussain, N., Jani, P.U., 1995. Nanoparticles as carriers for oral peptide absorption: studies on particle uptake and fate. *J. Control. Rel.* 36, 39–46.
- Gu, J.P., Robinson, J.R., Leung, S.H.S., 1988. Binding of acrylic polymers to mucin/epithelial surfaces: structure-property relationships. *Crit. Rev. Ther. Drug Carrier Syst.* 5, 21–67.
- Junginger, H.E., 1990. Bioadhesive polymer systems for peptide delivery. *Acta Pharm. Technol.* 36, 110–126.
- Kreuter, J., 1991. Peroral administration of nanoparticles. *Adv. Drug Deliv. Rev.* 7, 71–86.
- Lehr, C.M., Bouwstra, J.A., Tukker, J.J., Junginger, H.E., 1990. Intestinal transit of bioadhesive microspheres in an in situ loop in the rat: a comparative study with copolymers and blends based on poly(acrylic acid). *J. Control. Rel.* 13, 51–62.
- Lehr, C.M., Bouwstra, J.A., Kok, W., De Boer, A.G., Tukker, J.J., Verhoef, J.C., Breimer, B.B., Junginger, H.E., 1992. Effects of the mucoadhesive polymer polycarboxiphil on the intestinal absorption of a peptide drug in the rat. *J. Pharm. Pharmacol.* 44, 402–407.
- Longer, M.A., Ch'ng, H.S., Robinson, J.R., 1985. Bioadhesive polymers as platforms for oral controlled drug delivery, III. Oral delivery of chlorothiazide using a bioadhesive polymer. *J. Pharm. Sci.* 74, 406–411.
- Pimienta, C., Lenaerts, V., Cadieux, C., Raymond, P., Juhasz, J., Simard, M.A., Jolicoeur, C., 1990. Mucoadhesion of hydroxypropylmethacrylate nanoparticles to rat intestinal ileal segments in vitro. *Pharm. Res.* 7, 49–53.
- Riza, M., Tokura, S., Kishida, A., Akashi, M., 1994. Graft copolymers having a hydrophobic backbone and hydrophilic branches, part IX. Preparation of water-dispersible microspheres having polycationic branches on their surfaces. *New Polym. Mater.* 4, 189–198.
- Riza, M., Tokura, S., Iwasaki, M., Yashima, E., Kishida, A., Akashi, M., 1995. Graft copolymers having hydrophobic backbone and hydrophilic branches, X. Preparation and properties of water-dispersible polyanionic microspheres having poly(methacrylic acid) branches on their surfaces. *J. Polym. Sci. Polym. Chem.* 33, 1219–1225.
- Sakuma, S., Suzuki, N., Kikuchi, H., Hiwatari, K., Arikawa, K., Kishida, A., Akashi, M., 1997a. Oral peptide delivery using nanoparticles composed of novel graft copolymers having hydrophobic backbone and hydrophilic branches. *Int. J. Pharm.* 149, 93–106.
- Sakuma, S., Suzuki, N., Kikuchi, H., Hiwatari, K., Arikawa, K., Kishida, A., Akashi, M., 1997b. Absorption enhancement of orally administered salmon calcitonin by polystyrene nanoparticles having poly(*N*-isopropylacrylamide) branches on their surfaces. *Int. J. Pharm.* 158, 69–78.
- Sakuma, S., Ishida, Y., Sudo, R., Suzuki, N., Kikuchi, H., Hiwatari, K., Kishida, A., Akashi, M., Hayashi, M.,

- 1997c. Stabilization of salmon calcitonin by polystyrene nanoparticles having surface hydrophilic polymeric chains, against enzymatic degradation. *Int. J. Pharm.* 159, 181–189.
- Takeuchi, H., Yamamoto, H., Niwa, T., Hino, T., Kawashima, H., 1996. Enteral absorption of insulin in rats from mucoadhesive chitosan-coated liposomes. *Pharm. Res.* 13, 896–901.
- Yamaoka, K., Tanigawara, Y., Nakagawa, T., Uno, T., 1981. A pharmacokinetic analysis program (MULTI) for microcomputer. *J. Pharmacobio. Dyn.* 4, 879–885.